IOMAC'19

8th International Operational Modal Analysis Conference

2019 May12-14 Copenhagen

RESEARCH AND DEVELOPMENT OF AN AIR-PUFF EXCITATION SYSTEM FOR LIGHTWEIGHT STRUCTURES

Ben Halkon[1], Andreas Rauter[2], Sebastian Oberst[3] and Steffen Marburg[4]

[1] Dr, Centre for Audio, Acoustics & Vibration, University of Technology Sydney, Benjamin.Halkon@uts.edu.au.
[2] Mr, Mechanical Engineering, Technical University of Munich, Andreas.Rauter@tum.de.
[3] Dr, Centre for Audio, Acoustics & Vibration, University of Technology Sydney, Sebastian.Oberst@uts.edu.au.
[4] Prof., Mechanical Engineering, Technical University of Munich, Steffen.Marburg@tum.de.

ABSTRACT

Lightweight, thin-walled structures appear in numerous engineering and natural structures. Due to their sensitivity, vibration excitation by, now traditional, contacting techniques, such as modally-tuned impact hammers or electrodynamic shakers, to investigate their dynamics is challenging since it typically adds substantial mass and/or stiffness at the excitation location. The research presented in this article, therefore, is intended to yield a system for the non-contact excitation of thin-walled structures through small, controlled blasts of air. An air-puff system, consisting of two fast-acting solenoid-controlled valves, a small air outlet nozzle and bespoke control software with a programmable valve control sequence, is researched and developed. The excitation impulse characteristics are investigated experimentally and described in detail for varying input control parameters. Ultimately, suitability of the system for the excitation of thin-walled structures is explored, for both a 3D-printed micro-satellite panel and a natural bee honeycomb, with promising results when compared to that of an impact hammer.

Keywords: lightweight structures, non-contact excitation, air-puff system, dynamic characterisation

1. INTRODUCTION

Since the advent of commercially viable personal computers in the late ‘70s and their development through the proceeding decades, engineers and scientists have been able to research and develop increasingly sophisticated mathematical and numerical computation and modelling techniques applicable to a myriad of applications that have without doubt revolutionized the increasingly man-made environment in which we live. One such example of a technology that has enable engineers to concur previously insurmountable feats is that of structural analysis, in particular finite element analysis. With the monumental increase in the performance of readily accessible processing capacity, digital simulations of simplified real-world systems have become increasingly complex with often millions of degrees-of-freedom now used to predict the static and dynamic behaviour of engineered systems for a variety of load cases and boundary conditions. Indeed, the modern era has moved towards clusters of processing nodes and ‘cloud computing’ whereby model complexity and/or solution speed can be further increased by distributing solve jobs for parallel completion. In order to yield maximum value from such increasingly complex models, however, experimental correlation and validation remains necessary.

Historically such validation has been undertaken with traditional contacting transducers, such as accelerometers and strain gauges, and excitation techniques, such as modally tuned impact hammers or electrodynamic shakers. Such techniques are typically only able to offer practical equivalent models with on the order of ‘0s to ‘00s of degrees-of-freedom, with validation/correlation of increasingly complex models therefore presenting a challenge. Furthermore, such contacting characterization techniques also potentially introduce significant mass/stiffness modifications to the structure under test simply due to the physical attachment of a transducer of some form. This is particularly true for the case of, increasingly of interest, lightweight structures, where such modification can lead to significant changes in dynamic performance. There are methodologies for the mathematical removal of such mass/stiffness modifications from experiment results and, of course, the numerical computational models to be validated can be adjusted to include estimates of the corresponding experimental modifications. It is, however, preferable to not have to manage these complications, especially when developing practically applicable techniques that can be readily adopted by the industrial vibration engineer/CAE analyst. Furthermore, such methodologies for correction are only validated for engineering systems and can generally not be applied to natural structures of heterogeneous material composition and nonlinear dynamic behaviour.

In parallel with developments in computational performance and associated numerical techniques, the research and development of non-contact vibratory response measurement techniques has been of significant interest, largely driven by the inherent ability with such techniques to be able to rapidly generate high spatial resolution or, indeed, ‘whole-field’ structural vibratory response surveys. Technologies such as laser Doppler vibrometry [1] in particular, but also, for example, dynamic electronic speckle pattern interferometry (ESPI) [2] and photogrammetry/high-speed digital image correlation (DIC) [2],[3]. Research and development of such non-contact response measurement techniques has accordingly been followed by the concomitant need for non-contact excitation techniques, for example using pressurized air pulses, [4]-[6], by focused speaker [7] or speaker arrays [6],[8] or, for example, by high-power lasers using ablation or shock waves which are focused on the structure itself [9] to generate ultrasonic surface acoustic waves which can be used to determine damage in e.g. composites or in geological structures. Such experimental dynamic characterisation techniques are especially valid for the excitation of lightweight structures such as micro-satellite [10], (live) biological samples or insect appendages [11]. Delicate samples cannot, however, sustain the local elevated temperatures associated with high-power lasers, which would denaturalise protein and cause damage. A very low level of excitation, with no significant temperature increase, is required and, therefore, this paper addresses the research and development of a system, which makes used of a short duration air jet for such excitation.

2. AIR-PUFF EXCITATION SYSTEM RESEARCH AND DEVELOPMENT

2.1. Theoretical basis for the design of the air-puff system

The over-arching intention of the research described in this paper is to make use of a short impulsive jet of air to induce an excitation force into a lightweight, thin-walled structure, in a similar manner to that in which a traditional, modally-tuned instrumented impact hammer might. An attempt to apply governing fluid dynamics principles and equations to the problem as, a first approximation, could be made but it is anticipated that, in the limit at least and not least given that air is a compressible fluid, these governing principles may display limited validity on the scale of the system and structures concerned. Instead, drawing similarities between an air-puff system and an impact hammer, it is simply initially the intention to be able to control two parameters: i) the mass flow rate, considered to be proportional to the force generated, of the fluid through the nozzle and ii) the duration of the impulse.

Drawing hypothetical similarities between the proposed non-contact excitation system and that of the more traditional, contacting technique, the duration of the impact for an instrumented hammer directly controls the frequency range over which the structure is excited. Indeed, for a perfect Dirac delta impulse, the frequency range is infinite; for finite duration impulses, the longer the impact duration, the narrower the frequency range over which the structural response is excited. In an instrumented hammer excitation scenario, the duration of the impact is a function of the local combined stiffness of the hammer tip and that of the structure under test; this is adjusted as required by changing the hammer tip stiffness. In the case of the air-puff system described here, the duration of the impulsive jet of air will be controlled by a pair of fast operating pneumatic solenoid valves as described in what follows.

2.2. Description of the physical arrangement of the air-puff system

Figure 1 shows the experimental arrangement of the proposed air-puff system developed during this study. Two solenoid valves (Festo MHJ9-QS-4-MF) are mounted in series, from the laboratory compressed air supply, on an aluminium board, which includes different mounting options for the air-puff system. Specifically, these options are a ¼"-20 UNC thread for a camera tripod mount and a clamp for standard laboratory rods of ½" (12.7 mm) in diameter allowing for convenient positioning of the device. An electronic power supply (Elektro-Automatik EA-PSI 9040-40 T 1000W DC), allowing valve voltage adjustment between 12 and 53 V, is used to drive the solenoid valve control electronics module.

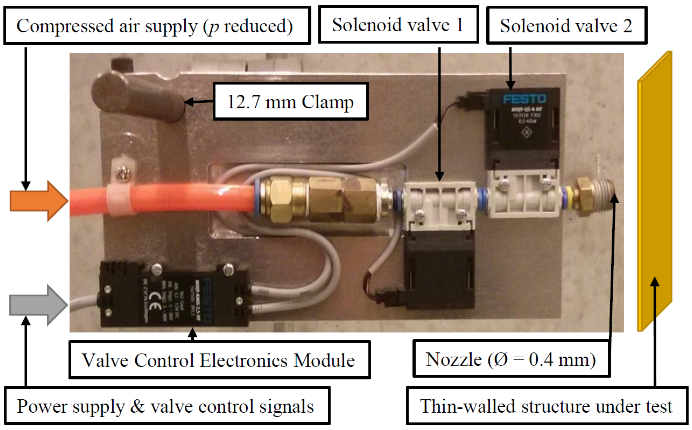

Figure 1. Experimental arrangement of the proposed air-puff system.

The reset mechanism utilized in the solenoid valves is that of an air spring for which the incoming pressurized air closes the valves when they are not activated by the solenoid. The pressurized air, adjustable between 0 and 7 bar, is assumed to be from an infinite volume source which maintains supply constant pressure during the operation of the air-puff system. Supply air pressure is adjusted using a pressure gauge, adjustable between 0.5 bar and 6 bar, upstream from the first valve. To achieve near point excitation and to excite small and sensitive structures, a small nozzle with an outlet diameter of 0.4 mm leads to an air jet at the front end of the air-puff system. A bespoke National Instruments LabVIEW-based control system was developed to enable control of the valve opening and closing.

2.3. Electromechanical characterisation of the air-puff system

2.3.1. Experimental methodology

In the GUI of the valve control software, the opening/closing sequence for the solenoid valves can be specified. Each valve is controllable individually by setting a sequence of up to eight open or close signals and the time duration for the segments. As can be seen in Figure 2, the typical sequence employed, so as to minimise the resulting impulse duration, is one whereby valve 2, that furthest downstream and thereby closest the structure under test, is open initially while valve 1 is initially closed. Shortly after opening valve 1, allowing the air to flow, valve 2 is closed, leading to a short duration puff of air. Sometime thereafter, and in advance of requiring a second pulse to excite the structure again, valve 1 can be closed and valve 2 opened. The entire cycle can then be repeated for a second "impact".

The first air-puff system control parameter, the overlap time duration, $\Delta t_{overlap}$, can thereby be specified with the second control parameter being the input pressure, p_{input}, set by adjusting the pressure gauge previously described. The air-puff system performance is described with reference to these two control parameters. To characterize the air-puff system excitation experimentally, the impulse peak force $F_{I,peak}$ and impulse duration Δt_I, defined graphically in Figure 3, were captured for varying input control parameters. The experimental setup consisted of a piezoelectric force transducer (Dytran 1053V2) onto

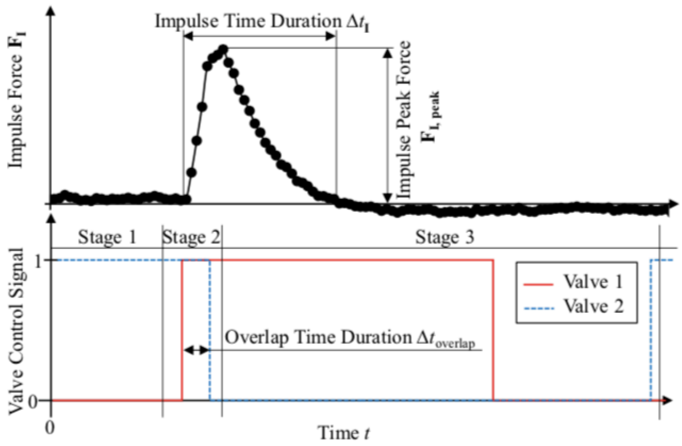

Figure 2. Typical valve control sequence showing control signals and example resulting force profile.

which the air puff was directed with the stand-off distance between the nozzle and the surface of the force transducer being adjustable. The force transducer was attached to a heavy, stiff steel block using a screw-on magnet mount plus a thin layer of synthetic beeswax, the latter preventing the magnetic connection from bouncing in high frequency vibration and therefore from parasitic frequency content potentially falsifying the measurements. Due to its weight, stiffness and boundary conditions, the steel block is assumed rigid and immune to the level of force generated by the air-puff system.

A Brüel & Kjær Type 3053-B-120 (12 channel, 25 kHz input module) data acquisition system was used to digitise the analogue force signal measured by the piezoelectric force transducer. The valve input control signals were measured in parallel enabling the definition of additional performance parameters for example including those relating to timing differences between the valve openings and the impulse peak force. Brüel & Kjær Pulse Reflex was utilised to set-up the acquisition parameters and perform signal analysis. The trigger threshold was set for the force sensor, with a 24 ms pre-trigger included to enable the entire impulsive force signal to be captured. Each measurement was recorded for 0.8 s, with a 2.56 kHz sample frequency, yielding a bandwidth of 1 kHz with 1.25 Hz resolution, i.e. 800 lines.

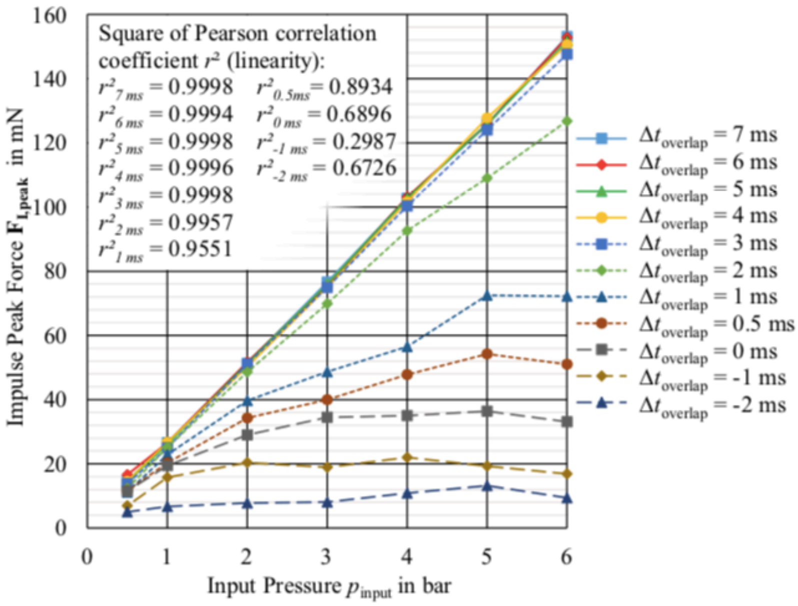

Figure 3. Impulse peak force vs. input pressure for varying valve opening overlap time duration.

2.3.2. *Experimental observations*

While the overlap time duration, $\Delta t_{overlap}$, and input pressure, p_{input}, were varied during the measurements, a valve control power supply of 50 V and a stand-off distance between the nozzle and the force transducer of 5 mm were specified and remained constant. Figure 3 shows the behaviour of $F_{I,peak}$ versus p_{input} for different $\Delta t_{overlap}$. A linear proportional relationship is visible for overlap time durations from 2 ms to 7 ms. To quantify the quality of the relationship, the square of the Pearson correlation coefficient (SPCC) r^2 is defined where $r^2 = 0$ means no correlation and $r^2 = 1$ confirms full linear correlation between the two parameters. For $\Delta t_{overlap}$ from 2 ms to 7 ms, the SPCC shows high values between 0.9957 and 0.9998. For $\Delta t_{overlap}$ from -2 ms to 1 ms, however, there is almost a step change in the performance characteristic with r^2 for a linear fit varying from 0.2987 to 0.9557. It is hypothesised that for valve behaviour for very short opening durations, loss effects within the system become significant with further investigation being required to fully confirm this behaviour.

As specified in Figure 2 previously, the second of the two air-puff parameters of interest in this application, the actual resulting impulse time duration, Δt_I, can also be determined and evaluated against the air-puff system input control parameters. Figure 4 shows this derived parameter against p_{input} and, again shows that, for $\Delta t_{overlap}$ from 2 to 7 ms, there appears to be a characteristic behaviour whereby Δt_I is at a minimum for p_{input} of 2 bar. Again, for $\Delta t_{overlap}$ of less than 2 ms, there is no apparent relationship.

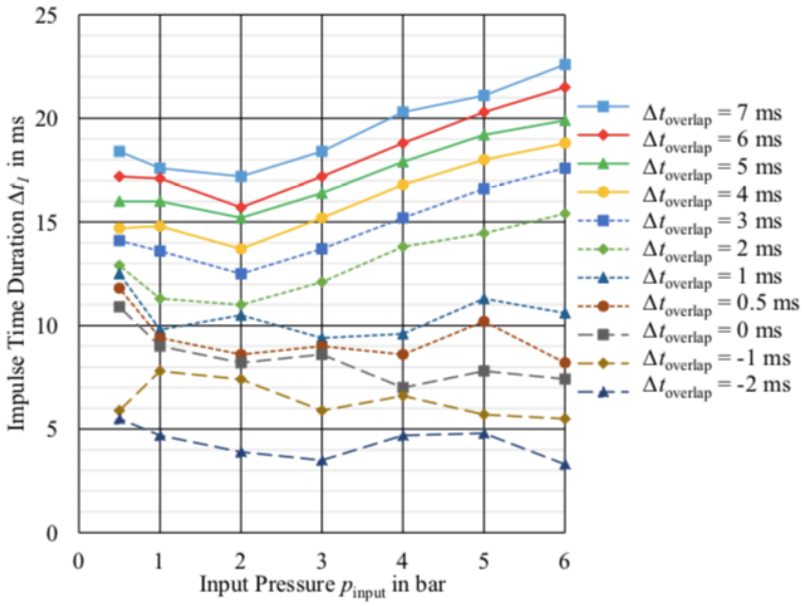

Figure 4. Actual impulse time duration vs. input pressure for varying valve opening overlap time duration.

The penultimate step of the benchtop characterisation of the air-puff system to be described is the example variation in $F_{I,peak}$ for varying the stand-off distance, $d_{stand\text{-}off}$ between the nozzle and the target; previously this was set to 5 mm. For this sub-investigation, p_{input} was set to 4 bar and $\Delta t_{overlap}$ to 1 ms. Figure 5 shows the interesting behaviour whereby, for the selected air-puff control system input parameters, $F_{I,peak}$ is a maximum at $d_{stand\text{-}off}$ 10 mm. The steep increase in $F_{I,peak}$ between 1 and 5 mm is evident. Further investigation is required to better characterise this behaviour for alternative air-puff system input control parameters; this will be the subject of future research and subsequent reporting.

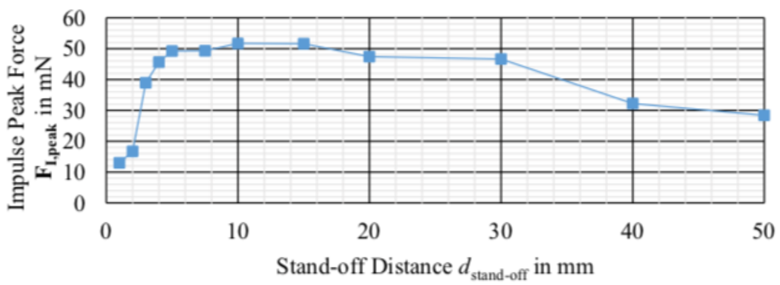

Figure 5. Impulse peak force vs. stand-off distance for 4 bar input pressure and 4 ms overlap time duration.

Lastly, a comparison of the impulsive force resulting excitation frequency spectrum achieved with a modally-tuned impact hammer (Brüel & Kjær Type 8204) with that of the air-puff system is presented in Figure 6. In this case, the air-puff system input parameters were again $p_{input} = 4$ bar, and $\Delta t_{overlap} = 1$ ms with $d_{stand\text{-}off}$ set to 5 mm. As shown in Figure 4, the resulting actual impulse force duration for these parameters is nominally 10 ms. The resulting frequency spectrum contains a "useful excitation range" (determined by a level of no less than one order magnitude lower than the peak) of up to c 233 Hz. In contrast, the impact hammer, complete with integral stainless steel tip, yielded an impact duration of 60 µs with the resulting excitation frequency spectrum being nominally flat across that range.

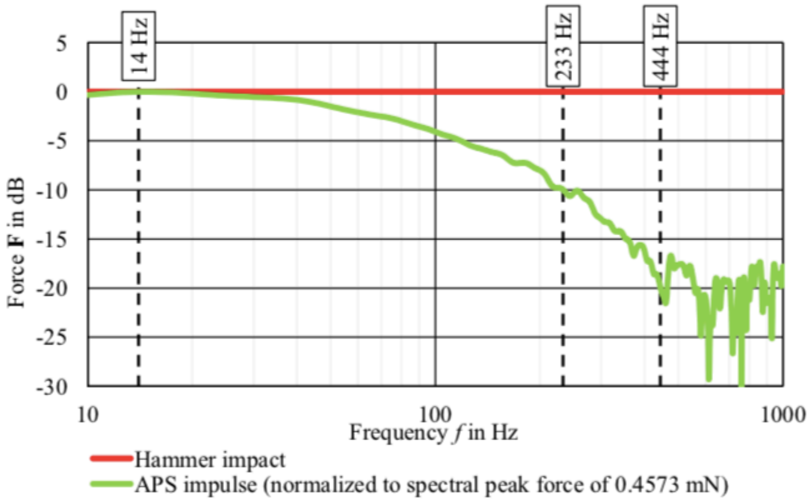

Figure 6. Comparison between impulse force for modally tuned impact hammer and air-puff system.

3. APPLICATION OF THE AIR-PUFF SYSTEM TO DYNAMIC CHARACTERISATION

To demonstrate the applicability of the air-puff system to structural dynamic characterisation, a pair of lightweight, thin-walled test specimens were evaluated. These were i) a 5 mm thickness, 100 x 100 mm ABS 3D-printed plate and ii) a bees' natural honeycomb structure. Comparisons between auto-power response only spectra for increasing numbers of averages are presented for excitation, either by modally tuned impact hammer (B&K Type 8204) or by the air-puff system. Both excitation, at a single point, and response accelerometer (Dytran 3225F), at an alternative single point, measurement locations were carefully chosen to attempt to excite the greatest number of structural resonances for comparison.

The first item under test described is a 3D-printed ABS plate weighing 51.7 g. It represents a multifunctional loadbearing panel from a cube micro-satellite and has a specific internal geometry intended to control the damping behaviour of the structure. Figure 7 shows the experimental arrangement. As can be observed therein, the ABS plate is "lightly suspended" on foam. This suspension arrangement enabled the collection of acceptable quality data for both excitation techniques with minimal change in the boundary conditions for each. For both excitation options, 0.64 s recordings were captured. For the air-puff system excitation, p_{input} = 6 bar, a $\Delta t_{overlap}$ = 1 ms (expected actual time impulse time duration approximately 10 ms based on Figure 4) and a $d_{stand\text{-}off}$ = 2 mm were arranged.

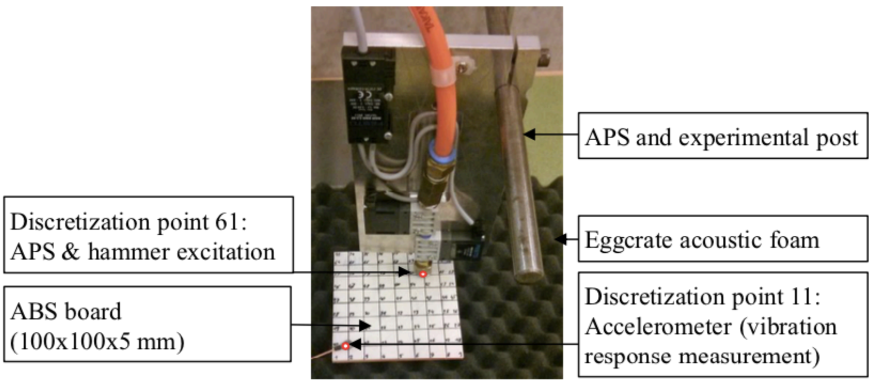

Figure 7. Experimental arrangement for ABS plate dynamic characterisation.

Figure 8 shows the correlation between the resulting auto-power spectra. Due to the relatively long impulse duration for the air-puff system vs. the impact hammer, it is expected that there is limited excitation energy above 250 Hz. Despite this, reasonable agreement between the resonant frequencies across the frequency can be observed. Indeed, at the lower frequencies and for data with multiple averages, the correlation is stronger. A future investigation would focus at the lower frequency range.

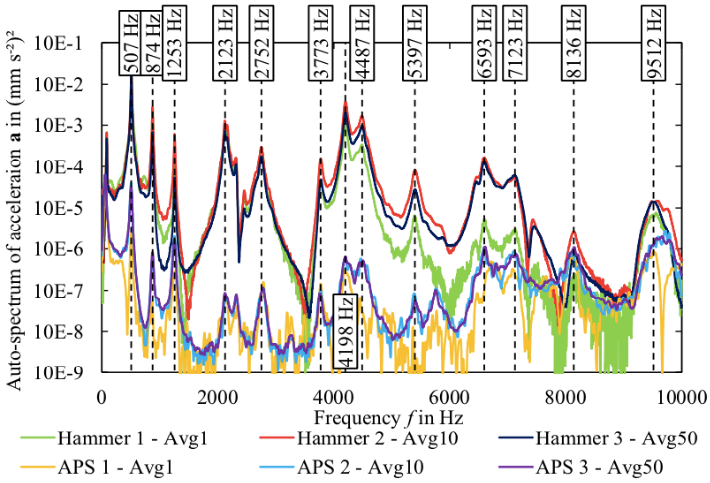

Figure 8. Comparison of response only auto-power spectra for ABS plate excitation.

The second item of interest under test is a natural bee honeycomb structure weighing only 1.2 g with approximate dimensions of 47 x 29 x 11 mm. Due to the very delicate nature of the item, the response measurement was made by a laser Doppler vibrometer orientated at 45 ° to the excitation direction in order to capture components of the response in two orthogonal directions. To minimise whole body motion of the structure, that would lead to significant challenges with making the response measurement due to the fixed probe laser beam orientation, the structure was mounted 'rigidly' to a block in a 'fixed-free' arrangement as shown in Figure 9. p_{input} = 6 bar, a $\Delta t_{overlap}$ = 0.5 ms (expected actual time impulse time duration 8 ms) and a $d_{stand\text{-}off}$ = 5 mm were arranged in this case for air-puff system excitation. Figure 10 shows the resulting auto-power spectra where agreement in the resonant frequencies of the structure is evident. There is particularly strong correlation between the techniques for 20 averages.

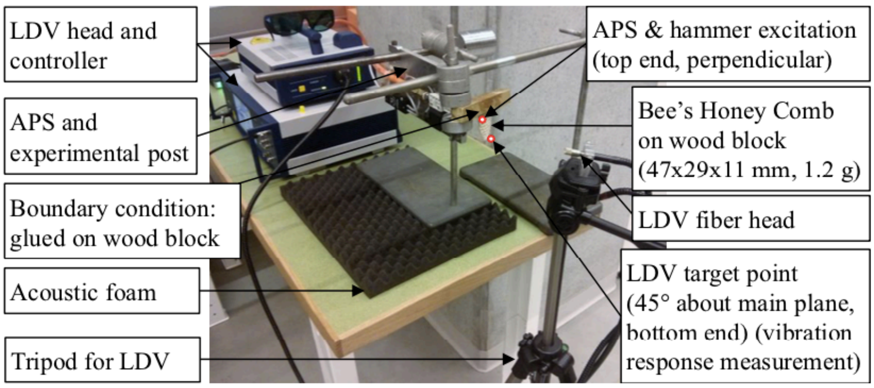

Figure 9. Experimental arrangement for bee honeycomb dynamic characterisation.

4. CONCLUSIONS

This paper has presented the research and development of a novel, fast-actuation pneumatic valve-based air-puff excitation system. The performance of the system for varying controllable parameters has been described and evaluated. Ultimately a comparison of the ability of the system to excited lightweight structures of interest has been presented with respect to a traditional, modally-tuned impact hammer equivalent technique with promising agreement observed, particularly at lower frequencies where the air-puff system is able to offer a reasonable level excitation. Future research will focus on the reduction of the pulse duration in order that a lower excitation level over a wider frequency range and a smaller excitation "spot" size might be realised. For this it is necessary to conduct a more comprehensive parameter and sensitivity study, to employ electro-magnetic values instead of mechanically opening solenoids and to explore tuning of the nozzle geometry. Whether filigree structures such as insect

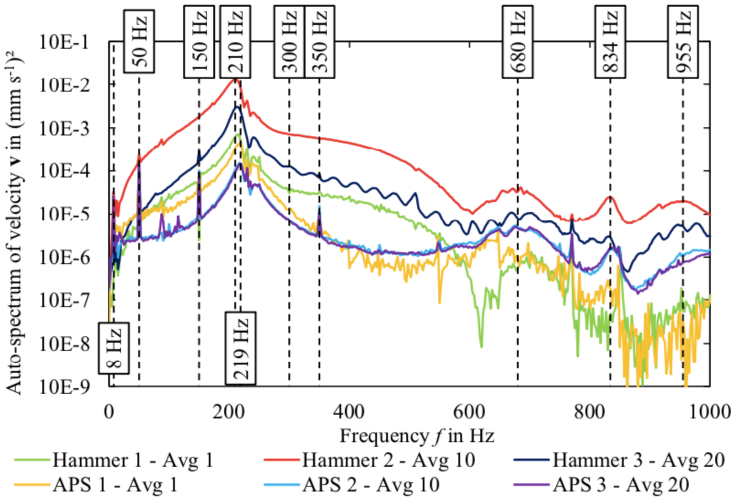

Figure 10. Example experimental arrangement of the air-puff system for dynamic characterisation.

appendages (legs, antennae, wings), expected to exhibit non-linear characteristics, can be sufficiently and carefully enough excited to determine their mechanical properties will be explored in the future.

ACKNOWLEDGMENTS

Andreas Rauter acknowledges the financial support provided by Sebastian Oberst through the UTS Centre for Audio, Acoustics and Vibration international visitor funds, enabling a visiting studentship to conduct the study. The authors wish to acknowledge the contribution made by Mr Chris Chapman, Scientific Officer, UTS to the development of the air-puff system hardware and software aspects.

REFERENCES

[1] Rothberg, S. et al. (2017). An international review of laser Doppler vibrometry: making light work of vibration measurement. *Optics and Lasers in Engineering*, 99, 11–22.

[2] Zanarini, A. (2019). Full field optical measurements in experimental modal analysis and model updating, *Journal of Sound and Vibration*, 442, 817-842.

[3] Baqersad, J., Poozesh, P., Niezrecki, C and Avitabile, P. (2017). Photogrammetry and optical methods in structural dynamics: A review, *Mechanical Systems and Signal Processing*, 86, 17-34.

[4] Vanlanduit, S., Daerden, F. and Guillaume, P. (2007). Experimental modal testing using pressurized air excitation. *Journal of Sound and Vibration*, 299, 83-98.

[5] Piraccini, M., Di Maio, D. and Di Sante, R. (2016). Nonlinear modal testing performed by pulsed-air jet excitation system. *Proceedings of the 34th IMAC, Vol.1*, 155-170.

[6] Farshidi, R., Trieu, D., Park, S.S. and Freiheit, T. (2010). Non-contact experimental modal analysis using air excitation and a microphone array. *Measurement*, 43, 755-765.

[7] Amraoui, Y.M. and Lieven, N.A.J. (2003). Noncontacting excitation and measurement of light structures. *Journal of Vibration and Acoustics*, 125, 114-119.

[8] Huber, T.M., Algren, M. and Raisbeck, C. (2016). Spatial distribution of acoustic radiation force for non-contact modal excitation. *Proceedings of the 34th IMAC, Vol.10,* 155–162.

[9] Hitchman, S., van Wijk, K. and Davidson, Z. (2016). Monitoring attenuation and the elastic properties of an apple with laser ultrasound. Postharvest Biology and Technology, 121, 71-77.

[10] Oberst, S. and Tuttle, S. (2018). Nonlinear dynamics of thin-walled elastic structures for applications in space, *Mechanical Systems and Signal Processing*, 110, 469-484.

[11] Oberst, S., Bann, G., Lai, J.C.S. and Evans, T.A. (2017). Cryptic termites avoid predatory ants by listening to their footsteps, *Ecology Letters*, 20, 212-22.